

# Modeling and Discussing an Interconnected Flux Magnetic Bearing

Domingos F. B. David<sup>1</sup>, José A. Santisteban<sup>1</sup>, and Afonso C. Del Nero Gomes<sup>2</sup>

<sup>1</sup>Departments of Mechanical and Electrical Engineering  
Universidade Federal Fluminense, Niteroi, Rua Passo da Pátria 156, CEP 20420-40, Brazil  
domingos@vm.uff.br, jasantisteban@vm.uff.br

<sup>2</sup>Department of Electrical Engineering  
Universidade Federal do Rio de Janeiro - CT, Rio de Janeiro, CEP 21945-970, Brazil  
nero@coep.ufrj.br

**Abstract** — An alternative idea for the construction of active magnetic bearings, adapted from a successful structure used in split-winding self-bearing motors, has been recently discussed in the literature. A mathematical model for this bearing configuration is developed in this paper. Preliminary theoretical results predict a greater equivalent stiffness for this model, when compared with traditional active magnetic bearings. The use of recently built prototypes for testing if these expectations hold true is also discussed.

**Index Terms** — Active magnetic bearings, interconnected magnetic flux, modeling.

## I. INTRODUCTION

Conventional active magnetic bearings (AMBs) [1], [2], [3], here called Type A, are based on the structure shown in Fig. 1. There are four “U-shaped electromagnets”, two for the x or horizontal direction and two in the y direction, resulting in four independent magnetic flux loops.

The windings in the x and y direction are fed with currents  $i_0 \pm i_x(t)$  and  $i_0 \pm i_y(t)$ ; the constant current  $i_0$  is the base, or bias, and the differential currents  $i_x$  and  $i_y$  will control the rotor position. Using basic reluctance concepts, the resultant forces  $f_x$  and  $f_y$  can be expressed in terms of these currents, the air magnetic permeability  $\mu_0$ , the total number of coils  $n_a$ , the cross section area in the stator ferromagnetic material  $A_a$  and the nominal length  $h$  of the air gaps. After a standard linearization procedure [1] around the operating point  $x = y = i_x = i_y$ , the forces generated by the Type A structure are shown in (1). Notice that the non connected nature of the magnetic fluxes leads to uncoupled forces:

$$\begin{cases} f_x = k_p^a x + k_i^a i_x \\ f_y = k_p^a y + k_i^a i_y \end{cases} \text{ where } \begin{cases} k_p^a = \mu_0 A_a n_a^2 i_0^2 / h^3 \\ k_i^a = \mu_0 A_a n_a^2 i_0^2 / h^2 \end{cases} \quad (1)$$

A different structure for magnetic bearings,

here named Type B, with four windings that cause interconnected magnetic loops, is depicted in Fig. 2.

This structure is found in the split-windings self-bearing motors researched in Brazil [4], [5]. In that approach, to provide spinning torques and radial restoring forces at the same time, alternate currents are injected in the windings; for the simpler case of AMBs, DC currents are considered.

Although other results are known with the Type B bearing concept [6], the authors of this article did not identify, up to now, the association of the interconnected flux structure with uncoupled equations for radial restoring forces or with higher values of the magnetic constants.

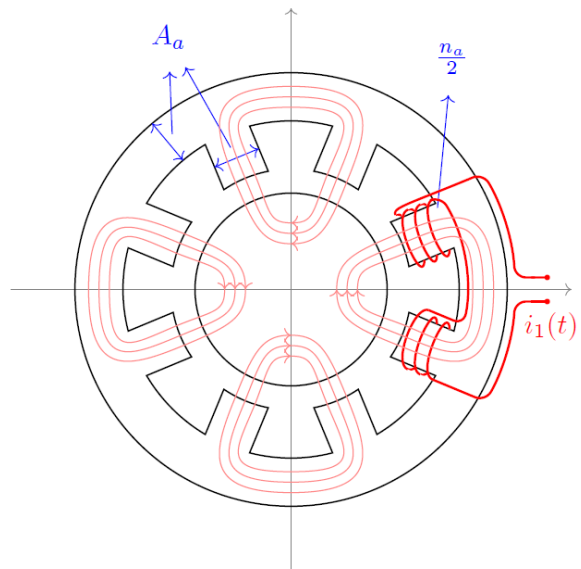


Fig. 1. Type A, or traditional, configuration for AMBs; windings are shown for the positive x (y) direction control the horizontal (vertical) position.

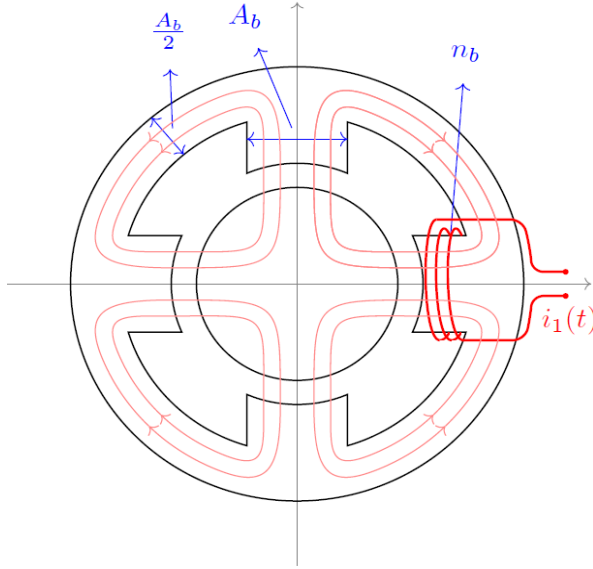


Fig. 2. Type B, the proposed configuration for AMBs; windings are shown for the positive  $x$  direction only; the flux paths are interconnected. Opposing pairs of windings along the  $x$  ( $y$ ) direction control the horizontal (vertical) position.

The generation of reluctance forces  $f_x$  and  $f_y$  in Type B bearings is detailed in Section II, which follows closely [7] and [8]. The linearized final expressions for these forces also show a decoupled nature, and the position and current constants,  $k_p^b$  and  $k_i^b$ , have higher values than in case A. Section III presents analytic results and simulations on how increasing  $k_{p,i}$  affects dynamic and control aspects of AMBs [8]. Details of the prototypes built to allow real comparisons between Types A and B, together with discussions about real tests, final comments and considerations on what remains to be done are made in Sections IV and V.

## II. FORCE GENERATION IN TYPE B BEARING

A detailed study of the force generation in the flux interconnected structure was presented in [4], [7] and [8]; the main points are repeated below. The  $x$  and  $y$  components of a radial displacement of the rotor change the nominal gap width  $h$  as shown in Fig. 3.

To compensate the displacements, it is usual to apply differential currents [1] to the pairs of windings: the differential, or control, currents  $i_x(t)$ , for the  $x$  or horizontal direction, and  $i_y(t)$ , for the vertical direction, are added and subtracted to a base, or bias, current  $i_0$ , a constant DC level. The total current, imposed at each

winding are:

$$i_1(t) = i_0 + i_x(t), i_3(t) = i_0 - i_x(t), \text{ at the } x \text{ axis, (2)}$$

$$i_2(t) = i_0 + i_y(t), i_4(t) = i_0 - i_y(t), \text{ at the } y \text{ axis. (3)}$$

Light pink lines in Fig. 2 represent the magnetic flux distribution caused by these currents. The reluctance forces depend on the total magnetic fluxes  $\Phi_k$ ,  $k = 1, 2, 3, 4$ , in the four air gaps with cross section area  $A_b$ :

$$f_x = \frac{\Phi_1^2 - \Phi_3^2}{2\mu_0 A_b} \quad \text{and} \quad f_y = \frac{\Phi_2^2 - \Phi_4^2}{2\mu_0 A_b}. \quad (4)$$

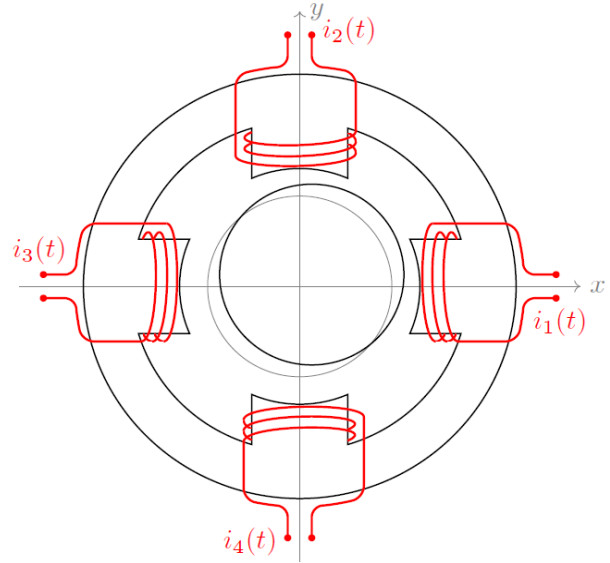


Fig. 3. When the rotor moves  $x$  and  $y$  in the horizontal and vertical positions, the air gap widths change to  $h - x$  in the right pole,  $h + x$  (left pole),  $h - y$  (upper pole) and  $h + y$  (lower pole); the fluxes are not shown.

The ferromagnetic connections in Type B allow a current injected in any winding to cause fluxes in all four air gaps; Fig. 4 illustrates the effects of  $i_1$  in all four “poles”. If  $\Phi_{jk}$  denotes the flux in air gap  $j$  caused by a current in winding  $k$ , the total magnetic flux  $\Phi_1$  in “pole” 1 depends on  $\Phi_{11}$ ,  $\Phi_{12}$ ,  $\Phi_{13}$ ,  $\Phi_{14}$ . Assuming no air or ferromagnetic losses, and positive signs for fluxes headed to the rotating center, the total magnetic fluxes in the poles are:

$$\Phi_1 = \Phi_{11} + \Phi_{12} - \Phi_{13} + \Phi_{14}, \quad (5)$$

$$\Phi_2 = -\Phi_{21} - \Phi_{22} - \Phi_{23} + \Phi_{24}, \quad (6)$$

$$\Phi_3 = -\Phi_{31} + \Phi_{32} + \Phi_{33} + \Phi_{34}, \quad (7)$$

$$\Phi_4 = -\Phi_{41} + \Phi_{42} - \Phi_{43} - \Phi_{44}. \quad (8)$$

For the determination of the sixteen values of  $\Phi_{jk}$ , let the magneto-motive generated by current  $i_1$  be denoted by  $F_1$  and the reluctances of the air gaps in the four poles in Fig. 3 by  $R_1$ ,  $R_2$ ,  $R_3$  and  $R_4$ . Figure 5 shows the equivalent circuit.

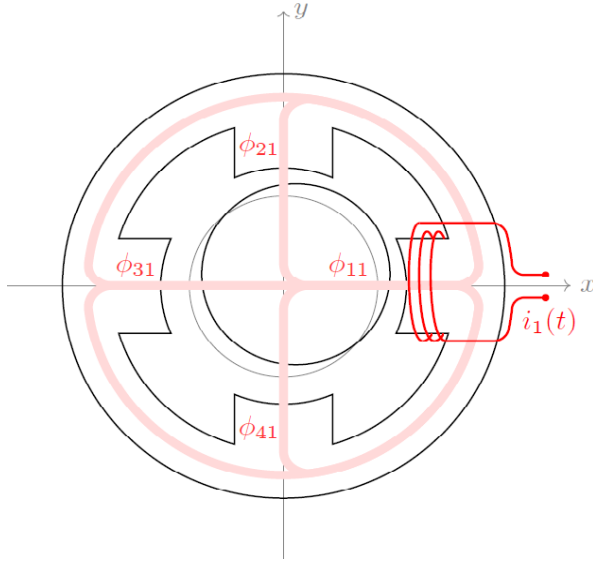


Fig. 4. Magnetic flux distribution associated to  $i_1$  in type B magnetic bearing; current injected only in winding 1 causes fluxes in all air gaps.

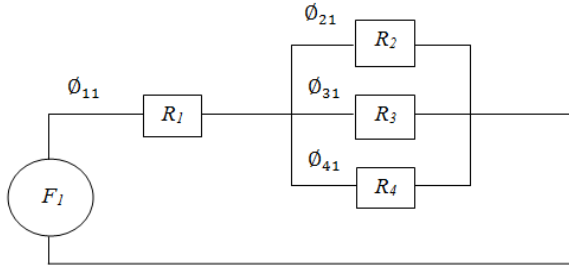


Fig. 5. Magnetic flux equivalent circuit associated to current only in winding 1 of type B magnetic bearing.

In the following development,  $A_b$  is the cross section area of the poles in Fig. 2. Considering that the reluctances are:

$$R_1 = \frac{h-x}{\mu_0 A_b}; R_2 = \frac{h-y}{\mu_0 A_b}; R_3 = \frac{h+x}{\mu_0 A_b}; R_4 = \frac{h+y}{\mu_0 A_b}; \quad (9)$$

the equivalent reluctance  $R_1^e$  can be found to be:

$$R_1^e = \frac{R_1 R_2 R_3 + R_1 R_2 R_4 + R_1 R_3 R_4 + R_2 R_3 R_4}{R_2 R_3 + R_2 R_4 + R_3 R_4}. \quad (10)$$

To avoid cumbersome formulas, the following auxiliary variables are defined:

$$N = R_1 R_2 R_3 + R_1 R_2 R_4 + R_1 R_3 R_4 + R_2 R_3 R_4, \quad (11)$$

$$D_1 = R_2 R_3 + R_2 R_4 + R_3 R_4, \quad (12)$$

$$D_2 = R_1 R_3 + R_1 R_4 + R_3 R_4, \quad (13)$$

$$D_3 = R_1 R_2 + R_1 R_4 + R_2 R_4, \quad (14)$$

$$D_4 = R_1 R_2 + R_1 R_3 + R_2 R_3. \quad (15)$$

Since  $F_1 = n_b i_1$ , algebraic operations lead to expressions for the fluxes associated to  $i_1 = i_0 + i_x$  imposed to the winding in pole 1 of Fig. 3:

$$\Phi_{11} = \frac{F_1}{R_1^e} = n_b (i_0 + i_x) \frac{D_1}{N}, \quad (16)$$

$$\Phi_{21} = n_b (i_0 + i_x) \frac{R_3 R_4}{N}, \quad (17)$$

$$\Phi_{31} = n_b (i_0 + i_x) \frac{R_2 R_4}{N}, \quad (18)$$

$$\Phi_{41} = n_b (i_0 + i_x) \frac{R_2 R_3}{N}. \quad (19)$$

The same procedure, repeated for currents  $i_2, i_3, i_4$  imposed at the windings in poles 2, 3 and 4, in Fig. 3, results in:

$$\Phi_{12} = n_b (i_0 + i_y) \frac{R_3 R_4}{N}; \quad \Phi_{22} = n_b (i_0 + i_y) \frac{D_2}{N};$$

$$\Phi_{32} = n_b (i_0 + i_y) \frac{R_1 R_4}{N}; \quad \Phi_{42} = n_b (i_0 + i_y) \frac{R_1 R_3}{N};$$

$$\Phi_{13} = n_b (i_0 - i_x) \frac{R_2 R_4}{N}; \quad \Phi_{23} = n_b (i_0 - i_x) \frac{R_1 R_4}{N};$$

$$\Phi_{33} = n_b (i_0 - i_x) \frac{D_3}{N}; \quad \Phi_{43} = n_b (i_0 - i_x) \frac{R_1 R_2}{N};$$

$$\Phi_{14} = n_b (i_0 - i_y) \frac{R_2 R_3}{N}; \quad \Phi_{24} = n_b (i_0 - i_y) \frac{R_1 R_3}{N};$$

$$\Phi_{34} = n_b (i_0 - i_y) \frac{R_1 R_2}{N}; \quad \Phi_{44} = n_b (i_0 - i_y) \frac{D_4}{N}.$$

The total fluxes  $\Phi_k$  for  $k = 1, 2, 3, 4$  can be determined by substituting the previous values of the partial fluxes  $\Phi_{jk}$  in Equations (5) to (8). Then, with the help of (4), the total reluctance forces generated in Type B magnetic bearing can be expressed as:

$$f_x = \frac{\mu_0 A_b n_b^2}{2} q_x(h, x, y, i_0, i_x, i_y), \quad \text{and} \quad (20)$$

$$f_y = \frac{\mu_0 A_b n_b^2}{2} q_y(h, x, y, i_0, i_x, i_y), \quad (21)$$

where  $q_{x,y}$  are the following functions:

$$q_x(h, x, y, i_0, i_x, i_y) = \frac{N_1^2 - N_2^2}{\Delta^2}, \quad \text{and} \quad (22)$$

$$q_y(h, x, y, i_0, i_x, i_y) = \frac{N_3^2 - N_4^2}{\Delta^2}, \quad (23)$$

with:

$$N_1 = (i_1 + i_2)\Delta_1 + (i_1 - i_3)\Delta_2 + (i_1 + i_4)\Delta_3,$$

$$N_2 = (i_3 - i_1)\Delta_2 + (i_2 + i_3)\Delta_4 + (i_3 + i_4)\Delta_5,$$

$$N_3 = (i_1 + i_2)\Delta_1 + (i_2 + i_3)\Delta_4 + (i_2 - i_4)\Delta_6,$$

$$N_4 = (i_1 + i_4)\Delta_3 + (i_3 + i_4)\Delta_5 + (i_4 - i_2)\Delta_6.$$

The currents  $i_k$  are defined in equations (2) and (3). If the distances  $h \pm x$  and  $h \pm y$  are denoted by  $\delta_x^\pm$  and  $\delta_y^\pm$ , the "Δs" values above are:

$$\Delta_1 = \delta_x^+ \delta_y^+, \quad \Delta_2 = \delta_y^+ \delta_x^-, \quad \Delta_3 = \delta_x^+ \delta_y^-,$$

$$\Delta_4 = \delta_x^- \delta_y^+, \quad \Delta_5 = \delta_x^- \delta_y^-, \quad \Delta_6 = \delta_x^+ \delta_x^-, \quad \text{and}$$

$$\Delta = \delta_x^- \delta_y^- \delta_x^+ + \delta_x^- \delta_y^- \delta_y^+ + \delta_x^- \delta_x^+ \delta_y^+ + \delta_y^- \delta_x^+ \delta_y^+.$$

In order to make the linearization of Equations (20) and (21), it should be considered that AMB's operate around a point  $P_0 = (x, y, i_x, i_y)_0 \cong (0, 0, 0, 0)$ . The partial derivatives in the vicinity of this point are:

$$\left. \frac{\partial q_x}{\partial x} \right|_{P_0} = \frac{4i_0^2}{h^3}, \quad \left. \frac{\partial q_x}{\partial y} \right|_{P_0} = 0, \quad (24)$$

$$\left. \frac{\partial q_x}{\partial i_x} \right|_{P_0} = \frac{4i_0^2}{h^2}, \quad \left. \frac{\partial q_x}{\partial i_y} \right|_{P_0} = 0. \quad (25)$$

If a similar procedure is made for  $q_y$ , the combined results lead to the linear expressions for the Type B structure forces:

$$\begin{cases} f_x = k_p^b x + k_i^b i_x \\ f_y = k_p^b y + k_i^b i_y \end{cases} \quad \text{where} \quad \begin{cases} k_p^b = 2\mu_0 A_b n_b^2 i_0^2 / h^3 \\ k_i^b = 2\mu_0 A_b n_b^2 i_0^2 / h^2 \end{cases}. \quad (26)$$

Two remarkable aspects are to be observed in Equation (26):

- (a) The complex interconnected fluxes in the Type B structure also lead to decoupled forces, in a similar way to Equation (1), derived for the Type A AMB's;
- (b) there is a factor 2 in Equation (26), when compared to Equation (1), derived for the Type A structure.

### III. THEORETICAL COMPARISONS

Assuming the same outside diameter of the stator, the following advantages can be identified for the Type B active magnetic bearing when it is compared with Type A:

- 1) The position and current constants  $k_p^b$  and  $k_i^b$  in Equation (26) are two times bigger than their counterparts  $k_p^a$  and  $k_i^a$  in Equation (1);
- 2) the cross section area  $A_b$  can be chosen greater than  $A_a$ ; it is reasonable to have  $A_b \approx 2A_a$ ;
- 3) the number of coils  $n_b$  can, possibly, be larger than  $n_a$ .

In conclusion the position ( $k_p$ ) and current ( $k_i$ ) constants for Type B AMBs have values at least 2 times higher than in case A. Depending on design aspects ( $A_b$  and  $n_b$ ), even higher rates can be achieved. How much can be these constants increased? The magnetic saturation seems to be the limit.

In order to evaluate the effects of  $k_p$  and  $k_i$  in an AMB performance, a theoretical analysis was applied in [8] to a simple control problem summarized in Fig. 6: a particle moving without friction in a horizontal and rectilinear path is to be positioned.

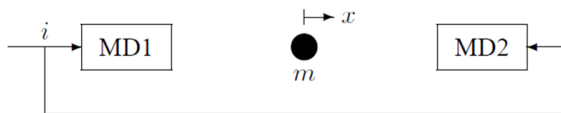


Fig. 6. The particle position  $x(t)$  is to be controlled by injecting currents in the magnetic devices MD1 and MD2.

The magnetic devices apply a horizontal force  $f(t) = k_p x(t) + k_i i(t)$  on the sphere, where  $i$  is a control current and  $x$  measures the displacement with respect to the reference position. A controller is desired, capable of driving the sphere position to 0 for all possible initial conditions  $x(0)$ , and in the eventual presence of constant, horizontal disturbance forces  $v$ . This is a simple, but meaningful, problem: many aspects of the real life operation and control of AMBs are present in it.

A stabilizing PD controller  $C(s) = as + \beta$  was designed; it ensured, as expected, that non zero initial displacements  $x(0)$  were corrected, when  $v = 0$ . When

a constant  $v$  was present, the controller effect lacked efficiency: the steady state offset error caused by such disturbances was found to be:

$$\rho = \frac{v_0}{\beta k_i - k_p}, \quad (27)$$

where  $v_0$  is the disturbance magnitude. The well known fact that PD controllers do not completely reject ( $\rho = 0$ ) constant disturbances becomes apparent. But Equation (27) tells more: for a fixed, stabilizing controller,  $\rho$  decreases when  $k_p$  and  $k_i$  increase by the same factor. In other words, if the position and current coefficients in a magnetic force generation law are both increased by the same amount, the resulting PD control is less sensitive to constant disturbances, and this characterizes a better, stiffer suspension.

In addition, it was simple to verify that a PID controller caused complete rejection of step disturbances, as expected, and that high or low values for the magnetic constants were not crucial in the stabilizing stage. But when constant disturbance rejection was needed, better transient behaviors were a direct consequence of higher  $k_p$  and  $k_i$  values.

The conclusions of the simple example in reference [8] are valid in much more general situations, involving real world applications of practical interest. And these conclusions are: increasing the values of the magnetic force constants  $k_p$  and  $k_i$  is a highly desirable goal in the AMB field.

### IV. PROTOTYPE BUILDING AND SIMULATIONS

The final conclusions of Sections II and III are that the interconnected fluxes in the Type B structure increase the values of the magnetic force constants  $k_p$  and  $k_i$ . How can one be sure about the theoretical tools used in those developments? The idea of the Type B structure has already been tested. In the prototype used at UFRJ [4], a vertical rotor is positioned in the radial directions by a self-bearing motor based on the interconnected fluxes of the Type B structure. This situation is more complicated, because the windings are fed with AC currents, to achieve the dual capabilities: torque generation and radial positioning. The device has worked!

The best possible way to give definite answers to the seminal questions posed above is by constructing prototypes and testing them in an exhaustive way. Only after this important stage, will the ideas proposed here be validated or not. Two prototypes, one for Type A and the other for Type B, have been constructed. Figure 7 shows a top view of them. A vertical rotor with a large, perforated upper disk will fill the above pieces; the same Fig. 7, in the center, shows a view of a mounted kit, with the rotor inserted in the casing with the stators.



Fig. 7. Top view of prototypes A, in the left and B in the right; notice the 8 “poles” in Type A, and only 4 “poles” in Type B. A mounted kit is shown in the center, with a vertical rotor inserted in one of the casings.

A finite element simulation of the magnetic characteristics of Type A and Type B structures [8] was done, and some results are shown below.

Figure 8 confirms the assumption that the flux generated at a particular winding is localized and does not interact with the other fluxes. Figure 9 shows clearly that a differential current in one direction does not affect the flux distribution in the other direction, thus confirming Equation (25).

The geometry of the flux lines, how they interconnect in Type B or remain isolated in Type A, confirms the basic assumptions used in Section II and on which this work relies.

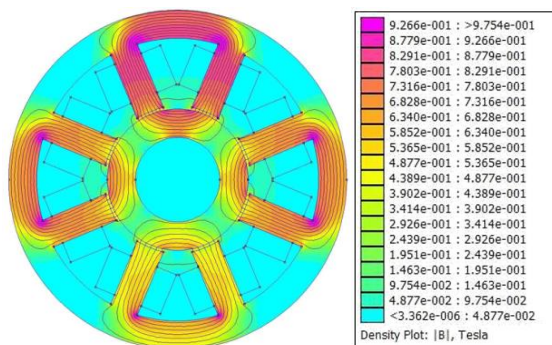


Fig. 8. Flux distribution in a Type A structure with balanced currents in the  $x$  axis and a differential current in the  $y$  direction.

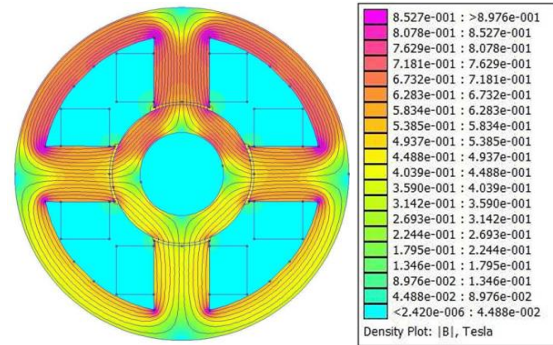


Fig. 9. Flux distribution in a Type B structure with balanced currents in the  $x$  axis and a differential current in the  $y$  direction.

A detailed mathematical model was built to describe the dynamic aspects of the prototypes. For evaluating their disturbance behavior, simulations were made when an extra mass was fixed in the upper disk. The rotor will be unbalanced by this and harmonic forces will be generated at the  $x$  and  $y$  axes. The resulting torques will disturb the centering capabilities of the most basic control laws used, imposing orbital movements to the rotor. This means that using the same initial conditions as before, the radial displacements will not tend to zero anymore. As expected, Type B behaves better than Type A in these extreme conditions; more details can be found in [9].

## V. COMMENTS AND CONCLUSIONS

The results in the previous section confirm the basic assumptions of Type B superiority on which this work relies. These are good news, but sound statements cannot be made yet: the prototypes are already finished but have not reached an operational stage yet. The laboratory tests are in a very primitive stage and no solid measurements has been made up to now. The authors have great expectations that the here called Type B concept will be a valid contribution for the active magnetic bearings field, because of the possibility of increasing their equivalent mechanical stiffness.

## REFERENCES

- [1] G. Schweitzer, H. Bleuler, and A. Traxler, *Active Magnetic Bearings*. Hochschulverlag AG an der ETH Zürich, 1994.
- [2] A. Chiba, T. Fukao, O. Ichikawa, M. Oshima, M. Takemoto, and D. Dorrel, *Magnetic Bearings and Bearingless Drives*. Newnes-Elsevier, 2005.
- [3] G. Schweitzer, E. Maslen, H. Bleuler, M. Cole, P. Keogh, R. Larsonneur, R. Nordmann, and Y. Ogada, *Magnetic Bearings: Theory Design and Applications to Rotating Machinery*. Springer-Verlag, 2009.
- [4] D. F. B. David, “Levitação de rotor por mancais-

motores radiais magnéticos e mancal axial sc auto-estável,” *D. Sc. Thesis*, COPPE-UFRJ, 2000.

- [5] E. F. Rodriguez and J. A. Santisteban, “An improved control system for a split winding bearingless induction motor,” *IEEE Transactions on Industrial Electronics*, vol. 58, no. 8, pp. 3401-3408, 2011.
- [6] L. Santos and K. Kjolhed, “Experimental contribution to high-precision characterization of magnetic forces in active magnetic bearings,” *Journal of Engineering for Gas Turbines and Power*, vol. 129, pp. 503, 2007.
- [7] D. F. B. David, J. A. Santisteban, and A. C. D. N. Gomes, “Interconnected four poles magnetic bearings,” in *Proceedings of the 1<sup>st</sup> Brazilian Workshop on Magnetic Bearings*, 2013. [www.magneticbearings2013.com.br](http://www.magneticbearings2013.com.br)
- [8] “Interconnected four poles magnetic bearings simulations and testing,” *Proceedings of ISMB14, 14th International Symposium on Magnetic Bearings*, pp. 30-35, 2014. <http://ismb14.magneticbearings.org>
- [9] “Laboratory tests on an interconnected four poles magnetic bearing,” in *Proceedings of ISMB15, 15th International Symposium on Magnetic Bearings*, 2016.



**Domingos F. B. David:** B.Sc. in Naval Engineering by the Federal University of Rio de Janeiro, in 1976; M.Sc. (1978) and D.Sc. (2000) in Mechanical Engineering from COPPE, at the same University. He has worked, until 1995, as Project Engineer dealing with equipments for the nuclear and chemical industries. Since then, he has been researching and teaching at the Mechanical Engineering Dept. of the Fluminense Federal University, Rio de Janeiro, Brazil.



**José A. Santisteban:** B.Sc. and Engineer degrees in Electronic Engineering from Universidad Nacional de Ingeniería (UNI), Lima, Perú, in 1986 and 1988, respectively, and the M.Sc. and D.Sc. degrees in Electrical Engineering from Universidade Federal do Rio de Janeiro (COPPE/UFRJ), Rio de Janeiro, Brazil, in 1993 and 1999, respectively. From 1988 to 1991, he was a Researcher and an Assistant Professor with UNI. From 1993 to 1995, he was a Researcher with UFRJ. In 1999, he joined the Fluminense Federal University, Niterói, Brazil, where he is currently an Associate Professor in

the Electrical Engineering Department acting in the Graduate Programs of Mechanical Engineering and the Electrical and Telecommunications Engineering. His current research activities include bearingless machines, power electronics, and electrical drives. He is a Member of the Brazilian Society of Power Electronics (SOBRAEP) and the Brazilian Society of Mechanical Engineering (ABCM). He is a co-author of the first Brazilian book on magnetic bearings.



**Afonso C. Del Nero Gomes:** B.Sc. in Aeronautical Engineering by ITA, the Aeronautical Technology Institute; M.Sc. and D.Sc. in Systems Engineering by COPPE in the Federal University of Rio de Janeiro, where he has been researching and teaching for undergraduate and graduate levels, for all his academic career.